

Informative Goodness-of-Fit for Multivariate Distributions

Sara Algeri¹

¹ School of Statistics, University of Minnesota,
0461 Church St SE, Minneapolis, MN 55455, USA.
Email: salgeri@umn.edu

Abstract

This article introduces an informative goodness-of-fit (iGOF) approach to study multivariate distributions. Conversely from standard goodness-of-fit tests, when the null model is rejected, iGOF allows us to identify the underlying sources of misspecification and naturally equip practitioners with additional insights on the underlying data distribution. The informative character of the procedure proposed is achieved by introducing the *joint comparison density*. As a result, the methods presented here naturally extend the seminal work of Parzen (1979) on univariate comparison distributions to the multivariate setting. Simulation studies show that iGOF enjoys high power for different types of alternatives.

Multivariate goodness-of-fit, informative inference, tests of independence, joint comparison density.

1 Introduction

The problem. In any experimental science, the knowledge available on a given phenomenon is typically formalized into a statistical model. The latter encapsulate our understanding of its nature, its properties as well as our uncertainties. Experimental measurements are then collected and statistical tests of hypothesis are used to answer the important question: *is our model valid?* When converting this scientific question into a statistical one, the *validity check* translates into the assessment of the properties characterizing the underlying data distribution. As a result, a variety of tests for goodness-of-fit (GOF) have been proposed in literature to investigate to study multivariate distributions.

For instance, let the measurements collected by the experiment be realizations of a random vector $\mathbf{X} = (X_1, \dots, X_p)$. Hotelling's T^2 test (e.g., Mardia, 1975) allow us to test the location parameter characterizing of the distribution of \mathbf{X} . In scientific terms, this translates into assessing if what we expect our measurements to be, on average, is a reasonable or not. Rank tests (e.g., Taskinen et al., 2005) can be used to assess independence, i.e., they help us understanding which aspects of the phenomenon are connected. Finally, classical univariate tests such as Kolmogorov-Smirnov (Kolmogorov, 1933; Smirnov, 1939) can be extended to the multivariate setting (e.g., Khmaladze, 2016) to validate arbitrary distributional assumptions, that is, assessing if our overall understanding of the phenomenon of interest is correct.

Despite their usefulness, these and similar GOF methods are somehow limited by their confirmatory nature. Specifically, when the respective null hypothesis is rejected,

they do not allow us to identify the underlying causes which invalidate the model postulated by the scientists, nor they give any indication on how the latter can be improved to obtain a closer representation of the true data distribution. In simple words, they do not provide any insights on *what went wrong*. As a result, this aspect is typically addressed by conducting a separate exploratory analysis followed by a (confirmatory) validity check for a newly postulated model.

Statistical goals. This article aims to bridge confirmatory and exploratory data analysis by introducing an informative approach to goodness-of-fit (iGOF). Specifically, iGOF targets three important questions arising in the statistical analysis of multivariate data:

- Q1. *Is the distribution of \mathbf{X} correctly specified and, if not, what are the sources of mismodelling?* For instance, are we misspecifying only some of the components of \mathbf{X} or is the problem affecting the entire random vector?
- Q2. *Are all the p components of \mathbf{X} independent and, if not, can we identify independent substructures?* As discussed in Section 4, the ability to address this question will not only allow us to characterize the dependence structure of \mathbf{X} , but it will also provide technical and computational advantages while investigating Q1.
- Q3. *How can we improve our postulated model?* Whatever the source of mismodelling is, either the dependence structure, the marginals or both, how can we provide a data-driven correction of our hypothesized model?

Finally, for the sake of generalizability, the underlying requirement of Q1-Q3 is to allow the components of \mathbf{X} to be either continuous or discrete.

Scientific motivations. While solutions for Q1-Q3 would enjoy a broad spectrum of applications across several scientific fields, the motivation of this work is rooted in the physical sciences. Interestingly, when converted in statistical terms, several issues arising in physics and astronomy naturally translate into Q1-Q3.

For instance, a common difficulty arising in the searches of new astrophysical phenomena, is the impossibility of correctly specifying the background distribution. In physics and astronomy, the “background” refers to all the astronomical objects or particles which are not those we aim to discover. Unfortunately, since many sources contribute to the background, its distribution is particularly difficult to model (e.g., [Priel et al., 2017](#); [Dauncey et al., 2015](#); [Algeri et al., 2018](#)). Investigating the validity of the hypothesized background models postulated by the scientists is a crucial step in many searches in physics and astronomy (Q1). Furthermore, when the hypothesized model is rejected, the possibility of identifying the source of mismodelling and provide adequate data-driven corrections (Q1,Q3) offers a notable advantage over the most popular methods proposed in literature to address this issue (e.g., [Yellin, 2002](#)).

When searching for new particles via colliders, another issues arising is the dependence among the kinematic variables involved. Unfortunately, their correlation is not always understood and therefore ignored (e.g., [Balázs et al., 2017](#)). Hence the need of

assessing the risk of ignoring the dependence structure (Q2) and, when not negligible, provide guidelines on how to model it (Q3). In this context, the measurements of kinematics variables (e.g., energy emission, number of jets in an event, number of leptons, etc) can have either continuous or discrete nature. Hence the need of providing a solution that could easily handle *mixed data* distributions.

The key elements of the solution. The comparison distribution has been popularized by the seminal work of Parzen (1979) as a valuable tool to perform goodness-of-fit. Specifically, let g_X , G_X , Q_{G_X} be, respectively, the hypothesized probability function, cumulative distribution function (cdf) and quantile function of a random variable X , either continuous or discrete, and we denote with f_X and F_X the true probability function and cdf. The *comparison density* between F_X and G_X Parzen (1979, 1983) can then be specified as

$$d(u; G_X, F_X) = \frac{f_X(Q_{G_X}(u))}{g_X(Q_{G_X}(u))} \quad \text{with } u = G_X(x), \quad (1)$$

and we assume $f_X = 0$ whenever $g_X = 0$. The *comparison distribution* is defined as $D(u) = \int_0^u d(s; G_X, F_X) ds$.

From (1) it is easy to see that the comparison density transparently models the departure of the hypothesized model and the true distribution. Its usefulness, however, is limited to the study of univariate distributions ($p = 1$). In this work, we overcome this limitation by introducing the *joint comparison density*. As it will become clear in the Sections to follow, the latter represents the key ingredient in addressing Q1-Q3.

Main results and organization. The core of the theoretical framework is presented in Section 2. Here, we define the *joint comparison density* and we propose its representation in terms of LP¹ score functions (e.g., Mukhopadhyay and Parzen, 2014; Mukhopadhyay and Wang, 2020). As shown in Sections 3 and 4, such representation substantially simplifies the subsequent stages of estimation, model selection and (post-selection) inference.

In Section 5, we propose the *dependence learning graph*, a valuable graphical tool to visualize the dependence structure of \mathbf{X} . As an important byproduct, the dependence learning graph also provides technical and computational advantages in the estimation of the joint comparison density.

In Section 6, we discuss an ANOVA-like testing strategy, which we call *iGOF-diagnostic analysis*, the latter is what allows us to assess the validity of the hypothesized model and, when rejected, identify the sources of mismodelling. Moreover, in support of the usefulness of iGOF, power studies are conducted via simulations in both Sections 4 and 6.

The main body of the article focuses on simple null hypothesis, that is, the postulated model is assumed to be fully specified. Extensions to situations where the null model depends on unknown parameters are discussed in Section 7.

¹In the LP acronym, the letter L typically denotes nonparametric methods based on quantiles, whereas P stands for polynomials (Mukhopadhyay and Wang, 2020, Supp S1).

As noted above, this work finds its main motivations in the context of astrophysical searches. Therefore, in Section 8 we illustrate how iGOF can be used to address the problem of mismodelling of the cosmic background considering a realistic simulation from the Fermi Large Area Telescope (Atwood et al., 2009).

Section 9 collects a summary of the results and a discussion of the limitations of iGOF. Technical proofs are collected in the Supplementary Material.

2 The joint comparison density

The univariate comparison density in (1) is also known in literature as *connector density* (e.g., Mukhopadhyay, 2017) in virtue of its ability to connect the true and the postulated model by means of the simple yet elegant decomposition

$$f_X(x) = g_X(x)d(G_X(x); G_X, F_X). \quad (2)$$

From (2), it is easy to see that if $G_X \equiv F_X$, then $d(u; G_X, F_X) = 1$ for all $u \in [0, 1]$. Conversely, if $G_X \not\equiv F_X$, $d(u; G_X, F_X)$ allows us to identify the regions of the support of X where f_X deviates substantially from g_X .

To exploit these useful properties in the multivariate setting, it is necessary to introduce a suitable definition of comparison density which extends to random vectors.

Definition 2.1 (The joint comparison density). *Let $f_{\mathbf{X}}$ and $F_{\mathbf{X}}$ be, respectively, the probability function and the cdf of $\mathbf{X} \in \mathcal{X} \subseteq \mathbb{R}^p$. Let $g_{\mathbf{X}}$ and $G_{\mathbf{X}}$ be the hypothesized probability function and cdf of \mathbf{X} , and such that, for every $\mathbf{x} = (x_1, \dots, x_p) \in \mathcal{X}$,*

$$g_{\mathbf{X}}(\mathbf{x}) = \prod_{d=1}^p g_d(x_d | \mathbf{x}_{<d}) \quad (3)$$

where $\mathbf{x}_{<d} = (x_1, \dots, x_{d-1})$ and g_1, \dots, g_p are suitable probability functions with associated cdfs and quantile functions G_d and Q_{G_d} , for all $d = 1, \dots, p$. Furthermore, assume that $f_{\mathbf{X}}(\mathbf{x}) = 0$ whenever $g_{\mathbf{X}}(\mathbf{x}) = 0$. The comparison density between $F_{\mathbf{X}}$ and $G_{\mathbf{X}}$ specifies as

$$d(\mathbf{u}; G_{\mathbf{X}}, F_{\mathbf{X}}) = \frac{f_{\mathbf{X}}(Q_{G_{\mathbf{X}}}(\mathbf{u}))}{g_{\mathbf{X}}(Q_{G_{\mathbf{X}}}(\mathbf{u}))} \quad (4)$$

with $\mathbf{u} = (u_1, \dots, u_p) = (G_1(x_1), \dots, G_p(x_p | \mathbf{x}_{<p})) = \mathbf{G}(\mathbf{x})$, $Q_{G_{\mathbf{X}}}(\mathbf{u}) = (Q_{G_1}(u_1), \dots, Q_{G_p}(u_p | \mathbf{u}_{<p}))$ and $\mathbf{u}_{<d} = (u_1, \dots, u_{d-1})$ for all $d = 1, \dots, p$.

In Definition 2.1, $\mathbf{u} = \mathbf{G}(\mathbf{x})$ is the equivalent of the Rosenblatt transformation (Rosenblatt, 1952) taken with respect to the postulated cdf $G_{\mathbf{X}}$. Notice that, in general, $\mathbf{G}(\mathbf{x}) \not\equiv G_{\mathbf{X}}(\mathbf{x})$ as $\mathbf{G}(\mathbf{x}) \in [0, 1]^d$ whereas $G_{\mathbf{X}}(\mathbf{x}) \in [0, 1]$. In the bivariate setting, for instance, one can choose $G_1 \equiv G_{X_1}$ and $G_2 \equiv G_{X_2|X_1}$, i.e., the hypothesized marginal cdf of X_1 and the hypothesized conditional cdf of $X_2|X_1$, respectively. Thus,

$$d(G_{X_1}(x_1), G_{X_2|X_1}(x_2|x_1); G_{X_1X_2}, F_{X_1X_2}) = \frac{f_{X_1X_2}(x_1, x_2)}{g_{X_1X_2}(x_1, x_2)} \quad (5)$$

or equivalently, in the quantile domain,

$$d(u_1, u_2; G_{X_1 X_2}, F_{X_1 X_2}) = \frac{f_{X_1 X_2}(Q_{G_1}(u_1), Q_{G_2}(u_2|u_1))}{g_{X_1 X_2}(Q_{G_1}(u_1), Q_{G_2}(u_2|u_1))}. \quad (6)$$

Remark 2.2. *The attentive reader may have noticed that, in principle, one could choose each $G_d \equiv G_{X_d}$, i.e., assuming independence among the components of \mathbf{X} . In this setting, (4) coincides with the copula density (e.g., Nelsen, 2007) of \mathbf{X} , whenever $G_{X_d} \equiv F_{X_d}$, for all $d = 1, \dots, p$ (see Section 5.1).*

The multivariate analogue of (2) follows directly from (4).

2.1 LP representation of comparison densities

While estimating (4) is an important goal of iGOF (see Q3 in Section 1), we also aim to provide a sufficiently detailed representation of the substructures characterizing the distribution of \mathbf{X} (see Q1 and Q2 in Section 1). To satisfy both these requirements, it is convenient to express the joint comparison density by mean of a suitable basis of orthonormal functions. For the sake of generalizability, a valuable requirement here to choose of a basis which easily generalizes to both discrete and continuous distributions. To serve this purpose, we construct a tensor product basis of LP score functions (e.g., Mukhopadhyay and Parzen, 2014; Mukhopadhyay and Wang, 2020).

When $p = 1$, a complete orthonormal basis of LP score functions in $L_2(G_X)$ can be specified by letting the first component to be $T_0(G_X(x)) = 1$. Subsequent components $\{T_j(G_X(x))\}_{j>0}$ are obtained by Gram–Schmidt orthonormalization of powers of

$$T_1(G_X(x)) = \frac{G_X^{\text{mid}}(x) - 0.5}{\sqrt{[1 - \langle p_{G_X}^3, 1 \rangle]/12}}, \quad (7)$$

where $p_{G_X}(x) = P(X = x)$ under the assumption that $X \sim G_X$, and $G_X^{\text{mid}}(x) = G_X(x) - 0.5p_{G_X}(x)$ is the so-called *mid-distribution function*, with mean 0.5 and variance $[1 - \langle p_{G_X}^3, 1 \rangle]/12$, respectively (Parzen, 2004). When X is continuous, $G_X^{\text{mid}}(x) = G(x)$ and $\langle p_{G_X}^3, 1 \rangle = 0$, consequently, the LP score functions reduce to normalized shifted Legendre polynomials. Whereas, when X is discrete, $\langle p_{G_X}^3, 1 \rangle = \sum_{x \in \mathcal{X}} p_{G_X}^3(x)$, with \mathcal{X} being the set of distinct points in the support of X .

For each G_d in Definition 2.1, we can then specify a basis of LP score functions, namely $\left\{ T_{j_d}(G_d(x_d | \mathbf{x}_{<d})) \right\}_{j_d \geq 0}$, such that

$$T_0(G_d(x_d | \mathbf{x}_{<d})) = 1 \quad (8)$$

$$T_1(G_d(x_d | \mathbf{x}_{<d})) = \frac{G_d^{\text{mid}}(x_d | \mathbf{x}_{<d}) - 0.5}{\sqrt{[1 - \langle p_{G_d}^3, 1 \rangle]/12}} \quad (9)$$

$$T_2(G_d(x_d | \mathbf{x}_{<d})) = \frac{\hat{T}_2(G_d(x_d | \mathbf{x}_{<d}))}{\|\hat{T}_2(G_d)\|}, \quad T_3(G_d(x_d | \mathbf{x}_{<d})) = \frac{\hat{T}_3(G_d(x_d | \mathbf{x}_{<d}))}{\|\hat{T}_3(G_d)\|}, \quad \dots \quad (10)$$

with

$$\hat{T}_{j_d}(G_d(x_d|\mathbf{x}_{<d})) = T_1^{j_d}(G_d(x_d|\mathbf{x}_{<d})) - \sum_{k=1}^{j_d-1} \langle T_1^{j_d}(G_d), T_k(G_d) \rangle T_k(G_d(x_d|\mathbf{x}_{<d})) \quad (11)$$

for all $j_d \geq 1$ and thus $\hat{T}_1(G_d(x_d|\mathbf{x}_{<d})) = T_1(G_d(x_d|\mathbf{x}_{<d}))$. In (8) and (11), the norms and inner products are taken with respect to the measure G_d . Proposition 2.3 follows from (8) and (11).

Proposition 2.3 (LP representation of the joint comparison density). *Let $S_{j_d}(u_d)$ be the equivalent of $T_{j_d}(G_d(x_d|\mathbf{x}_{<d}))$ expressed in the quantile domain, i.e.,*

$$S_{j_d}(u_d) = T_{j_d}\left(G_d(Q_{G_d}(u_d|\mathbf{u}_{<d})|Q_{G_1}(u_1), \dots, Q_{G_{d-1}}(u_{d-1}|\mathbf{u}_{<d-1}))\right) \quad (12)$$

with u_d, x_d, G_d and Q_{G_d} as in Definition 2.1. A square integrable joint comparison density over $[0, 1]^p$ can be expanded via a tensor product basis of LP score functions, i.e.,

$$d(\mathbf{u}; G_{\mathbf{X}}, F_{\mathbf{X}}) = \sum_{j_1, \dots, j_p \geq 0} \theta_{j_1, \dots, j_p} S_{j_1, \dots, j_p}(\mathbf{u}) \quad \text{with } \mathbf{u} \in [0, 1]^p \quad (13)$$

and $S_{j_1, \dots, j_p}(\mathbf{u}) = \prod_{d=1}^p S_{j_d}(u_d)$. The θ_{j_1, \dots, j_p} coefficients correspond to

$$\theta_{j_1, \dots, j_p} = \int_{[0, 1]^p} S_{j_1, \dots, j_p}(\mathbf{u}) d\mathbf{u}. \quad (14)$$

Proposition 2.3 can be easily verified by noticing that since each basis $\{S_{j_d}(u_d)\}_{j_d \geq 0}$ is orthonormal on $L_2[0, 1]$. Therefore, the functions $\{S_{j_1, \dots, j_p}(\mathbf{u})\}_{j_1, \dots, j_p \geq 0}$ form an orthonormal basis on $L_2[0, 1]^p$.

Remark 2.4. *By construction (see (8), (12)), the LP score functions are such that $S_{j_d}(\mathbf{u}) = 1$ whenever $j_d = 0$, for all $\mathbf{u} \in [0, 1]^d$ and $d = 1, \dots, p$. Therefore, $S_{0, \dots, 0}(\mathbf{u}) = 1$ for all $\mathbf{u} \in [0, 1]^p$ and $\theta_{0, \dots, 0} = 1$.*

3 Estimating comparison densities

Let $\mathbf{x}_1, \dots, \mathbf{x}_n$ be a sample of n i.i.d. observations from the random vector \mathbf{X} and let $\mathbf{U} = \mathbf{G}(\mathbf{X})$ be the respective Rosenblatt transformation (see Definition 2.1). Denote with $\mathbf{u}_1, \dots, \mathbf{u}_n$ the transformed sample with elements

$$\mathbf{u}_i = \mathbf{G}(\mathbf{x}_i) = (G_1(x_{1i}), \dots, G_p(x_{pi}|\mathbf{x}_{<pi})).$$

For analyses in dimensions larger than three, an important step is the specification of the Rosenblatt transformations $\mathbf{G} = (G_1, \dots, G_p)$ and which may substantially affect both the computational complexity and the accuracy of the method proposed. This aspect deserves careful consideration; therefore, we dedicate Section 5 to address it directly. Furthermore, here we implicitly assume that the postulated model, $G_{\mathbf{X}}$, is fixed and does not include any unknown parameter. Situations where the hypothesized models need to be estimated parametrically are covered in Section 7.

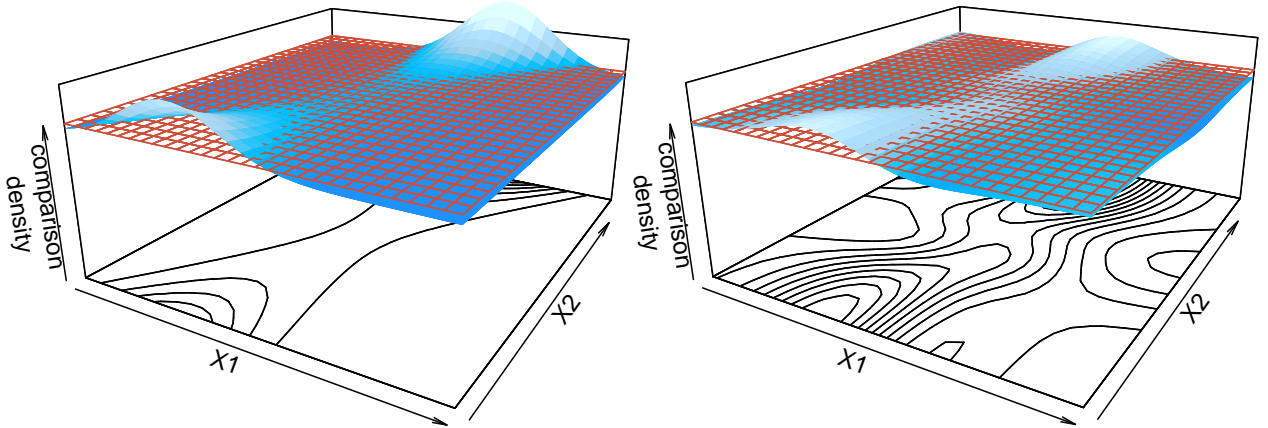


Figure 1: True and estimated comparison density for Example I. The left panel shows the comparison density of a random vector (X_1, X_2) distributed as a mixture of two, overlapping truncated bivariate Gaussians when the postulated model is assumed to be a bivariate truncated normal (see text). The respective estimate is shown in the right panel and is obtained via (18) with $m_1 = 4$ and $m_2 = 3$. The components of the $\hat{\boldsymbol{\theta}}$ vector have been selected via the AIC criterion in (30).

In (13), the summations involved are up to infinity when taken with respect to continuous X_d and up to $R - 1$ for discrete X_d , with R being the total number of distinct points in the support of X_d . However, to make the LP representation operational, it is necessary to truncate the series in (13) at points m_1, \dots, m_p . For the sake of simplifying the notation in this section and those to follow, let $M = \prod_{d=1}^p (m_d + 1) - 1$ and denote with $\boldsymbol{\theta}$ the $M \times 1$ vector of components $\theta_{j_1 \dots j_p}$, with j_1, \dots, j_p such that $\sum_{d=1}^p j_d \neq 0$, that is, $\boldsymbol{\theta}$ does not contain $\theta_{0 \dots 0}$ (see Remark 2.4). In a similar spirit, let $\boldsymbol{S}(\boldsymbol{u})$ be the $M \times 1$ vector of elements $S_{j_1 \dots j_p}(\boldsymbol{u})$ for all j_1, \dots, j_p such that $\sum_{d=1}^p j_d \neq 0$. Equivalently, denote with $\boldsymbol{T}(\boldsymbol{G}(\boldsymbol{x}))$ be the $M \times 1$ vector of elements $T_{j_1 \dots j_p}(\boldsymbol{G}(\boldsymbol{x}))$.

The parameter $\boldsymbol{\theta}$ can be estimated via its empirical counterpart $\hat{\boldsymbol{\theta}}$, i.e., the vector of components

$$\hat{\theta}_{j_1 \dots j_p} = \frac{1}{n} \sum_{i=1}^n S_{j_1 \dots j_p}(\boldsymbol{u}_i) \quad \text{for all } j_1, \dots, j_p \text{ such that } \sum_{d=1}^p j_d \neq 0, \quad (15)$$

The mean and covariance matrix of $\hat{\boldsymbol{\theta}}$ estimators are provided by Proposition 3.1; its proof is provided in the Supplementary Material.

Proposition 3.1. Let $d(\boldsymbol{u}; G_{\boldsymbol{X}}, F_{\boldsymbol{X}})$ be the joint comparison density of the random vector \boldsymbol{U} , then

$$E[\hat{\boldsymbol{\theta}}] = \boldsymbol{\theta} \quad \text{and} \quad \text{Cov}(\hat{\boldsymbol{\theta}}) = \boldsymbol{\Sigma} \quad (16)$$

where $\boldsymbol{\Sigma}$ has diagonal elements $\frac{\sigma_{j_1 \dots j_p}^2}{n} = \frac{1}{n} V[S_{j_1 \dots j_p}(\boldsymbol{U})]$ and non-diagonal elements $\frac{\sigma_{j_1 \dots j_p, h_1 \dots h_p}}{n} = \frac{1}{n} \text{Cov}[S_{j_1 \dots j_p}(\boldsymbol{U}), S_{h_1 \dots h_p}(\boldsymbol{U})]$. Furthermore, if $F_{\boldsymbol{X}} \equiv G_{\boldsymbol{X}}$, the equalities

in (16) reduce to

$$E[\widehat{\boldsymbol{\theta}}] = \mathbf{0} \quad \text{and} \quad \text{Cov}(\widehat{\boldsymbol{\theta}}) = \frac{1}{n} \mathbf{I}_M, \quad (17)$$

where $\mathbf{0}$ is a $M \times 1$ zero vector and \mathbf{I}_M is an $M \times M$ identity matrix.

From Proposition 3.1, it follows that an estimate of (4) can be constructed as

$$\widehat{d}(\mathbf{u}; G_{\mathbf{X}}, F_{\mathbf{X}}) = 1 + \widehat{\boldsymbol{\theta}}' \mathbf{S}(\mathbf{u}), \quad (18)$$

and has variance

$$V[\widehat{d}(\mathbf{u}; G_{\mathbf{X}}, F_{\mathbf{X}})] = \mathbf{S}(\mathbf{u})' \boldsymbol{\Sigma} \mathbf{S}(\mathbf{u}). \quad (19)$$

Combining (2), (4) and (18) an estimate of $f_{\mathbf{X}}$ is

$$\widehat{f}_{\mathbf{X}}(\mathbf{x}) = g_{\mathbf{X}}(\mathbf{x}) \widehat{d}(\mathbf{G}(\mathbf{x}); G_{\mathbf{X}}, F_{\mathbf{X}}) \quad (20)$$

$$= g_{\mathbf{X}}(\mathbf{x}) [1 + \widehat{\boldsymbol{\theta}}' \mathbf{T}(\mathbf{G}(\mathbf{x}))] \quad (21)$$

Interestingly, (20) implies that the comparison density allows to obtain an estimate of $f_{\mathbf{X}}$ which incorporates the information carried by the hypothesized model $g_{\mathbf{X}}$. Furthermore, from Proposition 3.2, it follows that the closer $g_{\mathbf{X}}$ is to $f_{\mathbf{X}}$ in terms of squared normalized distance, the lower the bias of $\widehat{d}(\mathbf{u}; G_{\mathbf{X}}, F_{\mathbf{X}})$.

Proposition 3.2. *The integrated squared bias of (18) is*

$$\int_{[0,1]^p} \left(\frac{f_{\mathbf{X}}(Q_{G_{\mathbf{X}}}(\mathbf{u})) - g_{\mathbf{X}}(Q_{G_{\mathbf{X}}}(\mathbf{u}))}{f_{\mathbf{X}}(Q_{G_{\mathbf{X}}}(\mathbf{u}))} \right)^2 d\mathbf{u} - \boldsymbol{\theta}' \mathbf{1} \quad (22)$$

where $\mathbf{1}$ is a $M \times 1$ unit vector.

The estimate in (21) is essentially that of a smooth model (e.g., Rayner and Best, 1990), that is, a smoothed version of the true underlying probability function. Similarly to the smooth model proposed by Barton (1956) in the univariate setting, the estimator in (21) may lead to estimate that are not *bona-fide*, i.e, they may be negative not integrate/sum up to one. In this manuscript we focus on (21) mostly for the sake of mathematical convenience in deriving the inferential results of Section 4 and their simple implementation. Nonetheless, bona-fide estimators can be constructed similarly to the univariate case as described in Algeri and Zhang (2020).

In order to illustrate the estimation process, we consider the following example.

Example I. Let (X_1, X_2) be a random vector with support $\mathcal{X} = [5, 20] \times [0, 17]$. Suppose that the hypothesized distribution, $G_{X_1 X_2}$, is that of a truncated bivariate normal with mean vector (12, 8), variances 8 and 12 and covariance 2. Whereas, the true model, $F_{X_1 X_2}$, is a mixture involving also another truncated bivariate Gaussian with the same mean vector, variances 4 and 20, covariance 5, and mixture parameter 0.15. In order to estimate the comparison density, we set $G_1 \equiv G_{X_1}$ and $G_2 \equiv G_{X_2|X_1}$. The estimated joint comparison density, obtained over a sample of $n = 7,000$ observations,

is shown in the right panel of Figure 1; the true comparison density is plotted on the left panel of the same figure. Despite the estimate obtained appears to recover the main departures from uniformity, the contours highlight that the estimator is rather noisy. Therefore, it is important to investigate the properties of (18) to assess the significance of the deviations observed.

4 Inference and model selection

Definition 2.1 implies that testing if $F \equiv G$, is equivalent to test that $d(\mathbf{u}; G_{\mathbf{X}}, F_{\mathbf{X}}) = 1$ with probability one, i.e.,

$$\begin{aligned} H_0 : d(\mathbf{u}; G_{\mathbf{X}}, F_{\mathbf{X}}) &= 1 \quad \text{for all } \mathbf{u} \in [0, 1]^p && \text{versus} \\ H_1 : d(\mathbf{u}; G_{\mathbf{X}}, F_{\mathbf{X}}) &\neq 1 \quad \text{for some } \mathbf{u} \in [0, 1]^p. \end{aligned} \quad (23)$$

Furthermore, from Proposition 2.3 it is easy to see that $d(\mathbf{u}; G_{\mathbf{X}}, F_{\mathbf{X}}) = 1$ for all $\mathbf{u} \in [0, 1]^p$, whenever all the $\theta_{j_1 \dots j_p}$ coefficients, but $\theta_{0 \dots 0}$, are identically equal to zero. Therefore, in practice, we test

$$H_0 : \boldsymbol{\theta} = \mathbf{0} \quad \text{vs} \quad H_1 : \boldsymbol{\theta} \neq \mathbf{0}. \quad (24)$$

Notice that H_0 in (23) implies H_0 in (24), but the opposite is not true in general. Whereas, H_1 in (24) does imply H_1 in (23). With a little abuse of nomenclature, in this section and those to follow, we will refer to $G_{\mathbf{X}}$ as the “null model”. Furthermore, we will refer to H_0 in (23) when generically saying that a result is valid “under H_0 ”. Indeed, most of the results presented here, only require validity of the “milder” H_0 in (24). However, more often than not, our derivations will involve model selection, and thus, to avoid complicating the notation further by specifying different H_0 for the different models under consideration, we will simply refer to H_0 in (23), and which implies all the model-specific nulls.

To conduct our inference, we consider the so-called *deviance* test statistics

$$D = n\widehat{\boldsymbol{\theta}}'\widehat{\boldsymbol{\theta}}. \quad (25)$$

The asymptotic null distribution of the deviance is given in Theorem 4.1.

Theorem 4.1. *If H_0 is true, then*

$$\sqrt{n}\widehat{\boldsymbol{\theta}} \xrightarrow{d} N(\mathbf{0}, \mathbf{I}), \quad \text{as } n \rightarrow \infty \quad (26)$$

where $N(\mathbf{0}, \mathbf{I})$ denotes a standard multivariate normal distribution. Furthermore,

$$D \xrightarrow{d} \chi_M^2, \quad \text{as } n \rightarrow \infty, \quad (27)$$

where M is the length of $\widehat{\boldsymbol{\theta}}$.

Corollary 4.2 follows directly from Theorem 4.1.

Corollary 4.2. Denote with $\{\widehat{d}(\mathbf{u}; G_{\mathbf{X}}, F_{\mathbf{X}})\}$ the random field indexed by $\mathbf{u} \in [0, 1]^p$ with components as in (18). Under H_0 ,

$$\left\{ \frac{\widehat{d}(\mathbf{u}; G_{\mathbf{X}}, F_{\mathbf{X}}) - 1}{\sqrt{\frac{1}{n} \mathbf{S}(\mathbf{u})' \mathbf{S}(\mathbf{u})}} \right\} \xrightarrow{d} \mathbf{Z}(\mathbf{u}), \quad \text{as } n \rightarrow \infty, \quad (28)$$

where $\mathbf{Z}(\mathbf{u})$ denotes a Gaussian random field with mean zero, unit variance and covariance function

$$\text{Cov}(\mathbf{Z}(\mathbf{u}), \mathbf{Z}(\mathbf{u}^\dagger)) = \frac{\mathbf{S}(\mathbf{u})' \mathbf{S}(\mathbf{u}^\dagger)}{\sqrt{\mathbf{S}(\mathbf{u})' \mathbf{S}(\mathbf{u}) \mathbf{S}(\mathbf{u}^\dagger)' \mathbf{S}(\mathbf{u}^\dagger)}}. \quad (29)$$

The proofs of both Theorem (4.1) and Corollary (4.2) are given in the Supplementary Material.

At this stage, constructing inference on the basis of Theorem 4.1 and Corollary 4.2 would be tempting. However, to guarantee the validity of our results we must, for the moment, refrain our impulses to compute p-values and confidence regions and consider how a very practical aspect of our estimation strategy could effectively invalidate a naive inferential approach. Specifically, either via an automatic procedure or by visual inspection, chances are that, when estimating the joint comparison density in (18), a model selection procedure is going to be implemented. Unfortunately, when a model is selected by a pool of possibilities, such process introduces an additional source of variability and thus the resulting inference is automatically affected (e.g., Berk et al., 2013). Section 4.1 addresses this aspect directly.

4.1 Post-selection inference

The estimate of the joint comparison density considered so far involves up to M tensor basis functions $S_{j_1 \dots j_p}(\mathbf{u})$. Nonetheless, it is possible that not all of these terms are needed to capture the departures of $G_{\mathbf{X}}$ from $F_{\mathbf{X}}$ and indeed, it is often convenient to remove some of them in order to avoid unnecessary sources of noise. Various criteria have been proposed in literature for univariate comparison densities and smooth models (e.g., Mukhopadhyay, 2017; Algeri, 2020) (see also Rayner et al. (2009, Ch.10)) and which can be easily extended to the multivariate setting. Here, we focus on the approach of Ledwina (1994) and (Claeskens and Hjort, 2004) and which relies on the BIC and AIC criteria.

Let $\widehat{\theta}_{(k)}$ be the k^{th} largest $\widehat{\theta}_{j_1 \dots j_p}$ estimate in terms of magnitude, i.e., $\widehat{\theta}_{(1)}^2 \geq \widehat{\theta}_{(2)}^2 \geq \dots \geq \widehat{\theta}_{(M)}^2$. Select the K largest coefficients which maximize either

$$\text{BIC}(K) = \sum_{(k)=1}^K \widehat{LP}_{(k)}^2 - \frac{K \log n}{n} \quad \text{or} \quad \text{AIC}(K) = \sum_{(k)=1}^K \widehat{LP}_{(k)}^2 - \frac{2K}{n}, \quad (30)$$

and include only the respective terms in the (18) estimate of the comparison density. Clearly, the choice of BIC or AIC is arbitrary and, from a practical standpoint, the BIC tends to lead to smoother estimates than the AIC.

The selection rules in (30) compare M possible models assuming that each m_d , for $d = 1, \dots, D$ was fixed before the researcher looked at the data. However, if one was to repeat the selection process several times, considering different m_d values each time, the number of models under consideration would increase even further. Because of this, and as advocated in Berk et al. (2013), a post-selection inferential strategy should be general enough to cover situations where multiple attempts, either in terms of selection procedure adopted and/or visual inspection, are made. Furthermore, Berk et al. (2013, Section 4.6) show that, under such framework, the problem of post-selection inference can indeed be reduced to one of simultaneous inference. In a similar spirit, here we construct a simple post-selection correction, which allows us to perform valid post-selection inference (in terms of both tests of hypothesis and confidence regions) while imposing one main assumption, i.e.,

Assumption 4.3. *Either by visual assessment or data-driven procedures, none of the estimators of (4) considered at any point during the analyses, contained more than M^* terms.*

Notice that Assumption 4.3 is sufficiently general to allow researchers to “cherry-pick” their p-values, as far as they are honest in declaring their M^* . Under Assumption 4.3, it follows from Theorem 4.1 that valid post-selection inference can be constructed as in Corollary 4.4. The respective proof is provided in the Supplementary Material.

Corollary 4.4. *Let $\{\hat{d}_1, \dots, \hat{d}_{M^*}\}$ be a pool of possible estimators of (4) from which \hat{d} is selected under Assumption 4.3. Let K , $0 \leq K \leq M^*$, be the number of LP tensors basis functions in each \hat{d}_K . Denote with D_K the deviance of \hat{d}_K , so that $D = D_K$ whenever $\hat{d} = \hat{d}_K$. If*

$$D_K \preceq D_{M^*} \quad \text{for all } K = 0, \dots, M^* - 1, \quad (31)$$

a valid post-selection bound for the p-value to test (23) is

$$p\text{-value}_{adj} = P(\chi_{M^*}^2 > D_{obs}) \quad \text{as } n \rightarrow \infty, \quad (32)$$

where D_{obs} is the value of D observed.

In (31) the symbol “ \preceq ” indicates that the left-hand-side is stochastically lower or equal than the right-hand-side. Each D_K in Corollary 4.4 only involves the sum of the squares of the estimates $\hat{\theta}_{j_1 \dots j_p}$ of the coefficients $\theta_{j_1 \dots j_p} \in \hat{d}_K$. Therefore, condition (31) is verified whenever the models under comparison are nested within \hat{d}_{M^*} , as it is the case when relying on the selection rules in (30) with $M^* = M$.

The deviance test presented here is a generalization of classical smooth tests to the multivariate setting and when considering random vectors with mixed components from arbitrary (either continuous and/or discrete) distributions. It follows that, classical results on smooth tests also apply to our setting. Among these, Ledwina (1994) has shown that, under H_0 , the BIC rule in (30), always selects the first component (i.e., the BIC is maximized at $K = 1$) as $n \rightarrow \infty$. Hence, in this setting, the (post-selection) distribution of the deviance statistic converges to that of a χ_1^2 and (32) could, in principle, be

replaced by its less conservative counterpart $P(\chi_1^2 > D_{\text{obs}})$. For finite samples, however, any $K > 2$ may still be selected with non-zero probability under H_0 , and thus applying the χ_1^2 approximation may lead to a larger probability of type I error than the nominal one.

In order to go beyond the binary nature of decisions based on the p-value and grasp further insights on the deviations of $G_{\mathbf{X}}$ from $F_{\mathbf{X}}$, it is worth constructing adequate confidence bands for our estimate of the comparison density. This can be done, while accounting for post-selection adjustments, as in Corollary 4.5. The proof is given in the Supplementary Material.

Corollary 4.5. *Let $SE(\widehat{d}_K(\mathbf{u})|H_0)$ be the standard error of the estimator \widehat{d}_K under H_0 . If*

$$\sup_{\mathbf{u}} \left| \left\{ \frac{\widehat{d}_K(\mathbf{u}) - 1}{SE(\widehat{d}_K(\mathbf{u})|H_0)} \right\} \right| \preceq \sup_{\mathbf{u}} \left| \left\{ \frac{\widehat{d}_{M^*}(\mathbf{u}) - 1}{SE(\widehat{d}_{M^*}(\mathbf{u})|H_0)} \right\} \right| \quad \text{for all } K = 1, \dots, M^* - 1, \quad (33)$$

then valid (post-selection adjusted) $(1 - \alpha)\%$ confidence regions, under H_0 in (23), for $\widehat{d}(\mathbf{u})$ are

$$\left[1 - c_\alpha SE(\widehat{d}(\mathbf{u})|H_0), 1 + c_\alpha SE(\widehat{d}(\mathbf{u})|H_0) \right] \quad \text{for all } \mathbf{u} \in [0, 1]^p \quad (34)$$

with c_α such that

$$P\left(\sup_{\mathbf{u}} \left| \left\{ \frac{\widehat{d}_{M^*}(\mathbf{u}; G_{\mathbf{X}}, F_{\mathbf{X}}) - 1}{SE(\widehat{d}_{M^*}(\mathbf{u})|H_0)} \right\} \right| > c_\alpha \middle| H_0\right) = \alpha. \quad (35)$$

Also in this case, we may expect the stochastic ordering condition in (33) to hold when considering estimators \widehat{d}_K nested within \widehat{d}_{M^*} . In this setting, \widehat{d}_{M^*} has the same terms as any other \widehat{d}_K plus, eventually, additional ones. Therefore, \widehat{d}_{M^*} is the least smooth among all the estimators considered. Consequently, we expect that the random field resulting from \widehat{d}_{M^*} to have the largest probability of crossing the fixed level c_α .

In Corollary 4.5, the choice of constructing confidence regions under the null hypothesis is justified by the fact that the estimator in (18) is, in general, a biased estimator of (2.1) (see Proposition 3.2). As a result, confidence regions constructed around $\widehat{d}(\mathbf{u})$ could be shifted away from the true joint comparison density. Despite the bias cannot be easily quantified in a general setting, it can be shown to be equal to zero when H_0 in (24) is true, hence the validity of (34).

From a theoretical perspective, a non-trivial aspect in the construction of (34) is the estimation of the quantile c_α . Probabilities such (35) are known in literature as *excursion probabilities* (e.g., Adler, 2000). Despite excursion probabilities cannot be expressed in closed form, accurate approximations under mild conditions exist (e.g., Taylor and Worsley, 2008). For the case of $p = 2$, and letting \mathbf{X} be continuous, the probability in (35) can be approximated by

$$2(1 - \Phi(c_\alpha)) + \mathcal{L}_1 \frac{e^{-\frac{c_\alpha^2}{2}}}{\pi} + \mathcal{L}_2 \frac{e^{-\frac{c_\alpha^2}{2}}}{\sqrt{2\pi}^{3/2}} + O(\exp(-\gamma c_\alpha^2/2)), \quad \text{as } n \rightarrow \infty, \quad (36)$$

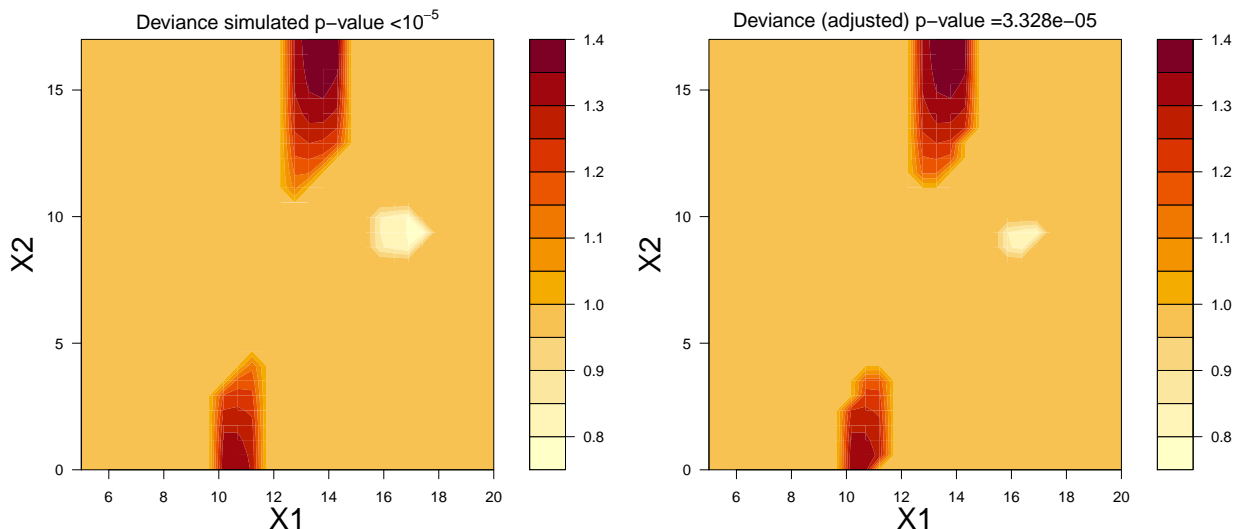


Figure 2: Simulated and approximated confidence regions for Example I. The left panel corresponds to the (post-selection) confidence regions and deviance p-value obtained via a simulation of size $B = 10,000$. The right panel shows to the (post-selection adjusted) confidence regions and deviance p-value computed as in (32) and (34). Darker shades correspond to significant deviations of the estimated comparison density above one. Lighter shades correspond to significant deviations below one.

for some $\gamma > 1$ (Taylor et al., 2005). In (36), \mathcal{L}_1 and \mathcal{L}_2 are constant known as Lipschitz-Killing curvatures and are typically estimated numerically (e.g., Algeri and van Dyk, 2020; Vitells and Gross, 2011).

As one may expect, despite Assumption (4.3), along with the stochastic ordering conditions in (31) and (33), guarantee wide applicability of the post-selection adjustments in (32) and (34), this advantage comes with a price. Specifically, they can be rather conservative for increasing values of M^* . Specifically, the larger m_d , p and M^* are, the more conservative our (post-selection) inference becomes. However, as shown below for Example I and in the sections to follow, in a relatively low-dimensional setting (32) still leads to high power even if the sample size is only moderately large. Similarly, (34) can be quite accurate and match closely the confidence regions obtained by simulating directly the distribution of (28), while repeating the selection process at each replicate.

Example I (continued). The comparison density estimate in the right panel of Figure 1 has been obtained by setting $m_1 = 4$ and $m_2 = 3$ and selecting the terms of the respective tensor basis via the AIC rule in (30). The resulting estimate is

$$\begin{aligned} \widehat{d}(G_1(x_1), G_2(x_2|x_1); G_{X_1 X_2}, F_{X_1 X_2}) = & 1 + 0.0339T_2(G_2(x_2|x_1)) - 0.0647T_2(G_1(x_1)) - 0.0206T_2(G_1(x_1)) \\ & + 0.0386T_{11}(G_1(x_1), G_2(x_2|x_1)) + 0.0281T_{13}(G_1(x_1), G_2(x_2|x_1)) - 0.0258T_{22}(G_1(x_1), G_2(x_2|x_1)) \\ & - 0.0235T_{31}(G_1(x_1), G_2(x_2|x_1)) - 0.0189T_{33}(G_1(x_1), G_2(x_2|x_1)) - 0.0180T_{43}(G_1(x_1), G_2(x_2|x_1)) \end{aligned}$$

	$n = 500$	$n = 1000$	$n = 2000$	$n = 5000$	$n = 7000$	$n = 10,000$
Type I error (\pm SE)	0.0540 (± 0.0023)	0.0500 (± 0.0022)	0.0499 (± 0.0022)	0.0482 (± 0.0021)	0.0508 (± 0.0022)	0.04930 (± 0.0022)
Power (\pm SE)	0.2157 (± 0.0041)	0.4456 (± 0.0050)	0.8063 (± 0.0040)	0.9995 (± 0.0002)	1.0000 (± 0.0000)	1.0000 (± 0.0000)

Table 1: Simulated probability of type I error and power for Example I considering different sample sizes. The nominal level is chosen to be $\alpha = 0.05$. Each simulation involves $B = 10,000$ replicates.

where $G_1 \equiv G_{X_1}$ and $G_2 \equiv G_{X_2|X_1}$. The AIC procedure selects 9 terms out of $M^* = M = 19$. The post-selection adjusted p-value and 95% confidence regions are shown in the right panel of Figure 2. The confidence contours are constructed by setting equal to one all the values of \hat{d} contained within the bands in (34). Whereas the quantile c_α has been calculated by solving

$$2(1 - \Phi(c_\alpha)) + \mathcal{L}_1 \frac{e^{-\frac{c_\alpha^2}{2}}}{\pi} + \mathcal{L}_2 \frac{e^{-\frac{c_\alpha^2}{2}}}{\sqrt{2}\pi^{3/2}} - \alpha = 0 \quad (37)$$

and estimating \mathcal{L}_1 and \mathcal{L}_2 by means of the R package TOHM (Algeri, 2019) as described in Algeri and van Dyk (2020). This approach led to $c_\alpha = 3.5424$. The confidence contours suggest that the most prominent deviations occur in correspondence of the regions $[10, 12] \times [0, 5]$ and $[12, 15] \times [12, 17]$. Here, the estimate of the comparison density shows significant deviations above one and thus we conclude that the postulated model underestimates the truth over these areas. The presence of significant departures of $G_{X_1 X_2}$ from $F_{X_1 X_2}$ are confirmed by the deviance test (adjusted p-value $\sim 3.328 \cdot 10^{-7}$). The left panel of Figure 2 shows the confidence regions and deviance p-value obtained by means of Monte Carlo simulations of $B = 10,000$. The selection procedure has been implemented for each simulated replicate. While more conservative, the confidence regions computed via (34) and (37), approximate reasonably well those obtained via simulation.

Finally, we investigate the probability of type I error and the power of the deviance test based on (32). Table 1 reports the results obtained considering a suite of five simulations, each of size $B = 10,000$, conducted using five different sample sizes. For all n considered, the probability of type I error observed is approximately the same than the nominal level $\alpha = 0.05$. Whereas, the power increases rapidly with n . For the smallest samples sizes considered, i.e., $n = 500$ and $n = 1000$, the power is rather low ($\sim 22\%$ and $\sim 45\%$, respectively). However, it has to be noted that, in our example, the mixture parameter is 0.15; therefore the deviations from the postulated model effectively account for only ~ 75 and ~ 150 data points when $n = 500$ and $n = 1000$, respectively.

5 Dependence learning and Rosenblatt transform

When the dimension of the problem increases, the specification of a postulated model $G_{\mathbf{X}}$, and the respective Rosenblatt transform (RT) in (2.1), may be challenging. The difficulty of this task is aggravated when limited knowledge on the overall dependence structure of \mathbf{X} is available.

To illustrate this aspect, let \mathbf{X} be a random vector with $p = 7$. A naive specification of the RT would be

$$G_7 \equiv G_{X_7|X_6, \dots, X_1}, G_6 \equiv G_{X_6|X_5, \dots, X_1}, \dots, G_2 \equiv G_{X_2|X_1}, G_1 \equiv G_{X_1}. \quad (38)$$

The RT in (38) implies that all the conditional distributions listed are known. In practice, however, even when a joint probability function $g_{\mathbf{X}}$ is available, deriving the conditionals in (38) from $g_{\mathbf{X}}$ may translate into a particularly burdensome computational task. In several physics experiments, for instance, the joint pdf $g_{\mathbf{X}}$ is not fully known analytically and some of its components can only be computed numerically (e.g., Balázs et al., 2017). In this setting, deriving the conditional distributions could involve expensive marginalizations and, even when derived, their evaluations on the data could be time consuming as each $u_{di} = G_d(x_{di}|\mathbf{x}_{<di})$ requires to evaluate G_d at points x_{1i}, \dots, x_{di} . The computational burden, however, can be mitigated by exploring the dependence structure and identifying independent sub-groups of variables within \mathbf{X} . For instance, if X_1, \dots, X_5 were independent from X_6, X_7 , then specifying G_7 as $G_{X_7|X_6}$ could substantially reduce the computational cost. Similarly, if X_1 and X_2 were independent, then G_2 could be set equal to G_{X_2} .

Notice that, in principle, one could choose $G_d \equiv G_{X_d}$ for all $d = 1, \dots, p$ and assume independence among the components of \mathbf{X} . However, there are situations where one would like to test the specific dependence structure specified in $G_{\mathbf{X}}$. Furthermore, for estimation purposes, omitting the dependence structure when available may affect substantially the bias of the estimators (see Proposition 3.2).

To address the need of learning the dependence structure of \mathbf{X} , in Sections 5.1 we discuss how or deviance (see Section 4) can be formulated as a test for independence and in Section 5.2 we introduce a practical graphical tool, called *the dependence learning graph*, which allows us to graphically identify independent sub-vectors of \mathbf{X} . Finally, simple criteria based on the dependence learning graph are identified to simplify the specification of the RT.

5.1 A deviance test for independence

As noted in Remark 2.2, when setting $G_d \equiv F_{X_d}$, for all $d = 1, \dots, p$, the joint comparison density reduces to the copula density, i.e.,

$$c_{\mathbf{X}}(F_{\mathbf{X}}(\mathbf{x})) = \frac{f_{X_1 \dots X_p}(x_1, \dots, x_p)}{f_{X_1}(x_1) \cdots f_{X_p}(x_p)} \quad (39)$$

Variable	True ($F_{\mathbf{X}}$)	Hypothesized ($G_{\mathbf{X}}$)	Correct
$X_6 X_1, X_2, X_5$	$\text{Poi}\left[e^{0.03x_1+0.02x_2+0.01x_2^2+0.02x_5}\right]$	$\text{Poi}\left[e^{0.03x_1+0.02x_2+0.02x_5}\right]$	No
X_1, X_2, X_5	$N\left[\left(\begin{pmatrix} 10 \\ 15 \\ 11 \end{pmatrix}, \begin{pmatrix} 4 & 0.5 & 0 \\ 0.5 & 3 & 1 \\ 0 & 1 & 5 \end{pmatrix}\right)\right]$	$N\left[\left(\begin{pmatrix} 10 \\ 15 \\ 11 \end{pmatrix}, \begin{pmatrix} 4 & 0.5 & 0 \\ 0.5 & 3 & 1 \\ 0 & 1 & 5 \end{pmatrix}\right)\right]$	Yes
$X_4 X_3$	Exponential $\left(\frac{1}{x_3}\right)$	Exponential $\left(\frac{1}{x_3}\right)$	Yes
X_3	Exponential(1)	Exponential(0.9)	No
X_7	T_3	Cauchy(0, 1)	No

Table 2: True and postulated model for Example II. The rows corresponds to the true and postulated models for each of the variables in the first column. The last columns highlights when mismodelling occurs.

which models directly the true dependence among the components of \mathbf{X} . A useful non-parametric estimator of $c_{\mathbf{X}}(F_{\mathbf{X}}(\mathbf{x}))$ has been proposed in recent literature by Mukhopadhyay and Parzen (2020). Interestingly, the latter can be framed as a special case of the approach presented in this manuscript. Specifically, in Mukhopadhyay and Parzen (2020), the copula density is estimated by setting $G_d \equiv \tilde{F}_{X_d}$, for all $d = 1, \dots, p$, with \tilde{F}_{X_d} being the empirical cdf of X_d . It follows that, in this setting, the deviance statistics in (25) reduces to a test for independence. Below, we illustrate this aspect considering pairwise dependence. Nonetheless, the framework presented below can be straightforwardly extended to test independence among groups of more than two variables (see Remark 6.3).

For each pair (X_d, X_l) , let $\tilde{\theta}_{ld}$ be the vector of components

$$\tilde{\theta}_{j_d j_l} = \frac{1}{n} \sum_{i=1}^n T_{j_d j_l}(\tilde{F}_{X_d}(x_{di}), \tilde{F}_{X_l}(x_{li})) \quad \text{with } j_d \in \mathcal{J}_d \text{ and } j_l \in \mathcal{J}_l \quad (40)$$

and $\mathcal{J}_d \subseteq \{1, \dots, m_d\}$, $\mathcal{J}_l \subseteq \{1, \dots, m_l\}$, i.e., if no selection rule is implemented, $\mathcal{J}_d \equiv \{1, \dots, m_d\}$ and $\mathcal{J}_l \equiv \{1, \dots, m_l\}$. From (39) we have that independence of X_d and X_l implies uniformity of the copula density. Hence we test

$$\begin{aligned} H_0 : c_{X_d X_l}(F_{X_d X_l}(x_d, x_l)) &= 1 \quad \text{for all } (x_d, x_l) \in \mathcal{X}_d \times \mathcal{X}_l && \text{versus} \\ H_1 : c_{X_d X_l}(F_{X_d X_l}(x_d, x_l)) &\neq 1 \quad \text{for at least one } (x_d, x_l) \in \mathcal{X}_d \times \mathcal{X}_l \end{aligned} \quad (41)$$

and a p-value to test (41) is

$$p_{ld} = P(\chi_{M_{ld}}^2 > D_{ld}) \quad \text{with } D_{ld} = n \tilde{\theta}'_{ld} \tilde{\theta}_{ld} \quad (42)$$

where $M_{ld} = m_d m_l$ is the maximum number of terms from which the components of $\tilde{\theta}_{ld}$ have been selected, i.e., we assume that $M^* = M_{ld}$ with M^* as in Assumption 4.3.

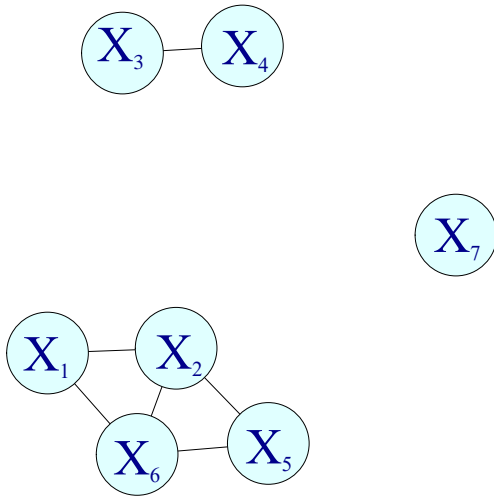


Figure 3: Dependence learning graph for Example II.

X_d	$\mathcal{G}_{(k)}$	$ E_d $	w_d	G_d
X_6	$\mathcal{G}_{(1)}$	3	10599.07	$G_{X_6 X_2, X_5, X_1}$
X_2	$\mathcal{G}_{(1)}$	3	10289.05	$G_{X_2 X_5, X_1}$
X_5	$\mathcal{G}_{(1)}$	2	740.73	G_{X_5}
X_1	$\mathcal{G}_{(1)}$	2	394.72	G_{X_1}
X_4	$\mathcal{G}_{(2)}$	1	3554.14	$G_{X_4 X_3}$
X_3	$\mathcal{G}_{(2)}$	1	3554.14	G_{X_3}
X_7	$\mathcal{G}_{(3)}$	0	-	G_{X_7}

Table 3: Rosenblatt transformations for Example II. Variables are conditioned only with respect to other variables in the same sub-graph. Variables with higher connectivity and stronger dependence are conditioned first.

Remark 5.1. The deviance statistics D_{ld} in (42) is the equivalent of the LPINFOR dependence measure proposed by Mukhopadhyay and Parzen (2020). The latter offers the rather unique advantage of quantify dependence (beyond linearity) among random variables, regardless of their discrete or continuous nature.

5.2 The dependence learning graph

In light of the results in Section 5.1, we can now construct the so-called *dependence learning graph*, a graphical tool to visualize the dependence structure of \mathbf{X} and, consequently, simplify the specification of the RT.

Definition 5.2 (The dependence learning graph). The dependence learning graph of \mathbf{X} is an undirected weighted graph, $\mathcal{G}_{\mathbf{X}} = (X_d, E_{dl}, w_{dl})$, with vertices the components of \mathbf{X} and edges E_{dl} such that X_d and X_l are joined by an edge if and only if p_{ld} in (42) is smaller than a predetermined significance level α . Each edge has weight $w_{dl} = D_{ld}$, with D_{ld} as in (42).

Notice that the dependence learning graph is a purely nonparametric tool which does not require any distributional assumption on the distribution of \mathbf{X} . When the overall dependence is unknown, $\mathcal{G}_{\mathbf{X}}$ allows us to identify possible substructures and guide practitioners in the specification of their postulated models $G_{\mathbf{X}}$ and the Rosenblatt transform $\mathbf{G}(\mathbf{x})$.

\mathbf{X}_q	df	(Adjusted) p-value
\mathbf{X}	16383	$< 10^{-130}$
(X_1, X_2, X_5, X_6)	256	$< 10^{-130}$
(X_1, X_2, X_5)	63	1
(X_3, X_4)	15	$1.799 \cdot 10^{-11}$
X_3	3	$3.801 \cdot 10^{-6}$
X_7	3	$3.732 \cdot 10^{-119}$

Table 4: *iGOF*-diagnostic table. The third column reports the (post-selection adjusted) deviance p-values for the test in (44) with \mathbf{X}_q specified as in the first column. The second column corresponds to the degrees of freedom used in the calculation of the p-value, i.e., the quantities M_q^* . The tests are ordered from the largest to the smallest sub-structure. The p-value in the first row is for the overall test in (24).

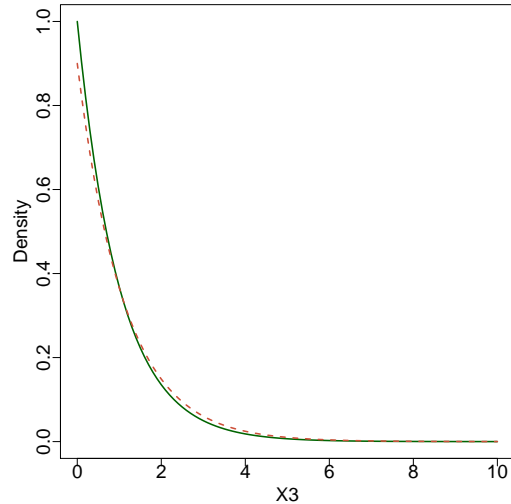


Figure 4: Comparing the postulated and the true model of X_3 . The green solid line corresponds to the probability density function (pdf) of an exponential random variable with unit rate. The red dashed line corresponds to the pdf of an exponential random variable with rate 0.9.

Specifically, let $\mathcal{G}_{(k)}$, $k = 1, \dots, K$, be the k^{th} largest disconnected sub-graph of $\mathcal{G}_{\mathbf{X}}$, so that each $X_d \in \mathcal{G}_{(k)}$ is disconnected from any $X_l \in \mathcal{G}_{(k')}$ for all $k \neq k'$. Denote with $|E_d|$ the degree of connectivity of each X_d i.e., the total number of edges connecting X_d to any other variable; whereas, w_d is the sum of the weights of each X_d , i.e., $w_d = \sum_l w_{dl}$. A parsimonious RT can then be specified according to the following criteria:

- (i) if G_d is a conditional cdf, the conditioning is only with respect to the components of \mathbf{X} belonging to the same sub-graph of X_d ;
- (ii) if G_d is a conditional cdf, the conditioning is only with respect to the components of \mathbf{X} with equal or lower connectivity than X_d ;
- (iii) among variables in the same sub-graph and with the same degree of connectivity, variables with higher weight w_d should be conditioned to variables with lower weight.

To illustrate these aspects we consider the following example.

Example II. We consider a sample of $n = 5000$ observations from a random vector $\mathbf{X} = (X_1, \dots, X_7)$ with components distributed as summarized in the second column of Table 2. Specifically, the sub-vector (X_1, X_2, X_5) is distributed as a bivariate normal, $X_6|X_1, X_2, X_5$ is Poisson distributed with rate depending on (X_1, X_2, X_5) . The variables (X_3, X_4) have joint pdf $f_{X_3X_4}(x_3, x_4) = \frac{1}{x_3} \exp(-x_3 - x_4/x_3)$ and thus $X_4|X_3 = x_3$ and

\mathbf{X}_q	Sample size (n)					
	500	1000	2000	3000	5000	10,000
\mathbf{X}	1	1	1	1	1	1
(X_1, X_2, X_5, X_6)	1	1	1	1	1	1
(X_1, X_2, X_5)	0	0	0	0	0	0
(X_3, X_4)	0.0070 (± 0.0008)	0.0356 (± 0.0019)	0.2492 (± 0.0043)	0.5927 (± 0.0049)	0.9580 (± 0.0020)	1
X_3	0.2461 (± 0.0043)	0.5701 (± 0.0050)	0.9164 (± 0.0028)	0.9906 (± 0.0010)	0.9998 (± 0.0001)	1
X_7	1	1	1	1	1	1

Table 5: Performance of the iGOF-diagnostic analysis for different sample sizes. The table shows the probabilities of rejection for each components when repeating the analysis in Table 4 $B = 10,000$ times, and using different sample sizes. For values different from zero and one the Monte Carlo errors ($\pm SE$) are also reported. The significance level considered is $\alpha = 0.05$.

X_3 are both exponentially distributed, with means x_3 and one, respectively. Finally, X_7 follows a T_3 distribution. It follows that (X_1, X_2, X_5, X_6) , (X_3, X_4) and X_7 are all independent from each other. Choosing $m_1 = \dots = m_7 = 3$, we estimate $\tilde{\boldsymbol{\theta}}$ as described in Section 5.1, and we select its components according to the BIC rule in (30). We proceed deriving the pairwise p-values in (42) and we construct the dependence learning graph $\mathcal{G}_{\mathbf{X}}$. The resulting graph is shown in Figure 3.

As expected, each of independent sub-group of variables forms a disconnected sub-graphs of $\mathcal{G}_{\mathbf{X}}$. Furthermore, since X_1 and X_5 are uncorrelated Gaussians (and therefore independent), despite they both belong to the largest sub-graph $\mathcal{G}_{(1)}$, they are not connected by an edge. Table 3 collects the RT obtained in accordance to (i)-(iii). Notice that since $\mathcal{G}_{(2)}$ contains only two variables, the RT can be equivalently specified by first conditioning X_4 to X_3 or vice-versa. Finally, since $\mathcal{G}_{\mathbf{X}}$ in Figure 3 suggests independence between X_1 and X_5 , we have $G_5 = G_{X_5|X_1} = G_{X_5}$.

6 iGOF-diagnostic analysis

The constructs introduced so far allow us to investigate the dependence structure of \mathbf{X} (Section 5), assess the validity of the postulated model $G_{\mathbf{X}}$ (Section 4) and obtain an estimate of the joint comparison density to visualize where and how departures of $g_{\mathbf{X}}$ from $f_{\mathbf{X}}$ occur (Section 3). Unfortunately, however, a visual inspection based on the comparison density is only possible when $p \leq 3$. Nevertheless, when $p > 3$, more insights on the sources of mismodelling affecting $G_{\mathbf{X}}$ can be obtained by conducting an ANOVA-like analysis where random sub-vectors of \mathbf{X} are tested individually, starting from the largest to the smallest. The underlying theory relies on the following theorem.

Theorem 6.1. *Without loss of generality, let $m_1 = \dots = m_p = m$ and assume that the components of $\hat{\boldsymbol{\theta}}$ have been selected under Assumption 4.3, with $M^* = (m + 1)^d - 1$, and*

assume that condition (31) holds. Let \mathbf{X}_q and $\mathbf{U}_q = \mathbf{G}_q(\mathbf{X}_q)$ be random vectors collecting $q \leq p$ components of \mathbf{X} and $\mathbf{U} = \mathbf{G}(\mathbf{X})$, respectively, and

$$g_{\mathbf{X}_q}(\mathbf{x}_q) = \prod_{h=1}^q g_h(x_h | \mathbf{x}_{<h}) \quad \text{for all } x_h \in \mathbf{x}_q. \quad (43)$$

Denote with $\widehat{\boldsymbol{\theta}}_q$ the sub-vector of $\widehat{\boldsymbol{\theta}}$ of elements $\widehat{\boldsymbol{\theta}}_{j_1 \dots j_p}$ with $j_d = 0$ for all d such that $X_d \notin \mathbf{X}_q$. As $n \rightarrow \infty$, a post-selection adjusted p -value to test

$$H_0 : G_{\mathbf{X}_q} = F_{\mathbf{X}_q} \quad \text{versus} \quad H_1 : G_{\mathbf{X}_q} \neq F_{\mathbf{X}_q} \quad (44)$$

is

$$p\text{-value}_{q,adj} = P(\chi_{M_q^*}^2 > D_q), \quad (45)$$

with $D_q = n\widehat{\boldsymbol{\theta}}_q' \widehat{\boldsymbol{\theta}}_q$ being the deviance statistics of \mathbf{X}_q and $M_q^* = (m+1)^q - 1$.

Theorem 6.1 follows directly from the orthogonality of the LP tensor basis functions $\{S_{j_1 \dots j_p}(\mathbf{u})\}_{j_1 \dots j_p \geq 0}$ for any \mathbf{X}_q satisfying (43).

Remark 6.2. Because of condition (43), Theorem 6.1 holds only for random sub-vectors of \mathbf{X} whose RT transform \mathbf{G}_q includes all the conditioning, from the higher to the lower, necessary to recover $g_{\mathbf{X}_q}(\mathbf{x}_q)$. To some extent, this condition can be seen as the iGOF counterpart of the marginality principle advocated by Nelder (1977) in the context of ANOVA.

Similarly to the ANOVA, Theorem 6.1 allows us to construct an iGOF-diagnostic table to identify the source of mismodelling for a given random vector \mathbf{X} . Below we show how this can be done for Example II.

Example II (continued). Consider once again our 7-dimensional random vector with components distributed as in Table 2. We are interested in testing the validity of the postulated model in the third column of Table 2. The RT is specified as in the fifth column of Table 3 and a deviance test has been constructed for each sub-graph $\mathcal{G}_{(k)}$ identified via the dependence learning plot. The results are collected in Table 4. The overall deviance test is reported in the first row and correctly reject the null model. Similarly, the test in the second row, rejects the hypotheses that the vector (X_1, X_2, X_5, X_6) is modelled correctly, and fails to reject the model for (X_1, X_2, X_5) . This aspect is particularly important as it highlights that the mismodelling occurs only with respect to the conditional distribution of $X_6 | X_1, X_2, X_5$. The tests in the fourth and fifth row show that the vector (X_3, X_4) has been mismodelled and one source of mismodelling is the marginal of X_3 . Ultimately, the test for X_7 also correctly rejects the null hypothesis of Cauchy distribution. Table 5 collects the results of a simulation obtained by repeating the diagnostic analysis in Table 4 through a simulation of $B = 10,000$ replicates, while considering different sample sizes. Even when the sample size considered is only 500, the most prominent deviations are captured with probability one, whereas, the model for (X_1, X_2, X_5) is never rejected. More issues arise in diagnosing mismodelling of X_3 and,

consequently, (X_3, X_4) for smaller samples. For instance, even when $n = 1000$ the power of the procedure in detecting departures of G_{X_3} from F_{X_3} is only $\sim 57\%$ and $\sim 3\%$ for (X_3, X_4) . It has to be noted, however, that detecting mismodelling of X_3 is a particularly challenging task. As shown in Figure 4, the postulated and the true pdf of X_3 are very close one-another; this minor differences are further “diluted” when considering the joint distribution of (X_3, X_4) , since $X_4|X_3$ is correctly specified. Nevertheless, such minor deviations are detected with high power for larger sample sizes.

Remark 6.3. From Remark 5.1 it follows that when setting $G_d \equiv \tilde{F}_{X_d}$, for all $d = 1, \dots, p$, our *iGOF*-diagnostic analysis reduces to an analysis of independence for groups of two or more variables.

7 Extensions to the parametric case

The methods discuss so far assume that the postulated model $G_{\mathbf{X}}$ is fully specified and it does not include free parameters to be estimated. For instance, $G_{\mathbf{X}}$ may have been specified on the basis of the results obtained from previous studies, it has been calibrated over multiple runs of the experiment or it has been estimated on a *training* set and *iGOF* is used to assess its validity on a *test* set. In many practical situations, however, $G_{\mathbf{X}}$ does depend on unknown parameters, which we denote with $\boldsymbol{\beta}$ and indeed, one of the main goals of many physics experiments is to test different models and set reliable limits on the so-called “systematic uncertainties”, i.e., the components of $\boldsymbol{\beta}$. Therefore, at this stage, a legitimate question is: *can we still use iGOF in this setting?* The answer is yes, if the procedure is adequately modified.

In order to discuss how this can be done in practice, here we focus on the case where the free parameter $\boldsymbol{\beta}$ is estimated via maximum likelihood; hence, we assume the usual regularity conditions (e.g., Cramér, 1999, p.500) hold. Specifically, let $\hat{\boldsymbol{\beta}}$ be the Maximum Likelihood Estimate (MLE) of $\boldsymbol{\beta}$, let $\mathbf{b}_{\boldsymbol{\beta}}(\mathbf{x})$ and $n\boldsymbol{\mathcal{I}}_{\boldsymbol{\beta}}$ be the score vector and the the Fisher information matrix, respectively, i.e.,

$$\mathbf{b}_{\boldsymbol{\beta}}(\mathbf{x}) = \frac{d}{d\boldsymbol{\beta}} \log g_{\mathbf{X}}(\mathbf{x}, \boldsymbol{\beta}) \quad \text{and} \quad \boldsymbol{\mathcal{I}}_{\boldsymbol{\beta}} = \frac{d^2}{d\boldsymbol{\beta}d\boldsymbol{\beta}} \log g_{\mathbf{X}}(\mathbf{x}, \boldsymbol{\beta}). \quad (46)$$

Moreover, let $\hat{\boldsymbol{\theta}}_{\hat{\boldsymbol{\beta}}}$ be the equivalent of $\hat{\boldsymbol{\theta}}$ in Section 3 obtained by replacing $\boldsymbol{\beta}$ with $\hat{\boldsymbol{\beta}}$ in $G_{\mathbf{X}}$. While one may expect the asymptotic distribution of $\hat{\boldsymbol{\theta}}_{\hat{\boldsymbol{\beta}}}$ to be the same as $\hat{\boldsymbol{\theta}}$, under H_0 , this is not true in general. Specifically, classical results on smooth tests (e.g., Thas, 2010, Sec 4.2.2.3 and 5.2.2.3) can be used to show that the null asymptotic distribution of $\sqrt{n}\hat{\boldsymbol{\theta}}_{\hat{\boldsymbol{\beta}}}$ is that of a zero-mean multivariate normal with matrix of variances and covariances given by

$$\boldsymbol{\Sigma}_{\hat{\boldsymbol{\beta}}} = \mathbf{I}_M - \boldsymbol{\Sigma}_{\mathbf{b}\boldsymbol{\beta}}\boldsymbol{\mathcal{I}}_{\boldsymbol{\beta}}^{-1}\boldsymbol{\Sigma}_{\boldsymbol{\beta}\mathbf{b}} \quad (47)$$

with M being the length of $\hat{\boldsymbol{\theta}}_{\hat{\boldsymbol{\beta}}}$, $\boldsymbol{\Sigma}_{\boldsymbol{\beta}\mathbf{b}}$ is the matrix of elements $\int_{\mathcal{X}} T_{j_1 \dots j_p}(\mathbf{G}(\mathbf{x})) b_{q\boldsymbol{\beta}}(\mathbf{x}) d\mathbf{G}(\mathbf{x})$ and $b_{q\boldsymbol{\beta}}$ is the q^{th} component of $\mathbf{b}_{\boldsymbol{\beta}}$ in (46).

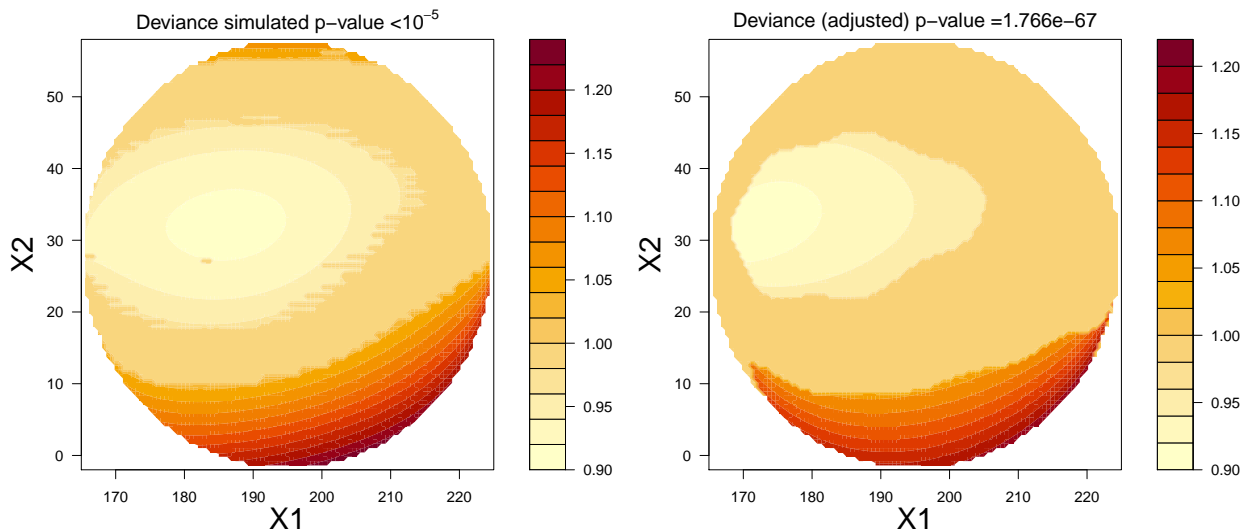


Figure 5: Simulated and approximated confidence regions for the Fermi LAT simulation. The left panel corresponds to the (post-selection) confidence regions and deviance p-value obtained via a simulation of size $B = 10,000$. The right panel shows to the (post-selection adjusted) confidence regions and deviance p-value computed as in (32) and (34). Darker shades correspond to significant deviations of the estimated comparison density above one. Lighter shades correspond to significant deviations below one.

Furthermore, since (47) is non-diagonal, the deviance statistics must be modified accordingly, and thus we write

$$D_{\hat{\beta}} = n\hat{\theta}'_{\hat{\beta}}\Sigma_{\hat{\beta}}^{-1}\hat{\theta}_{\hat{\beta}}. \quad (48)$$

By exploiting the results of Kallenberg and Ledwina (1997), the distribution of (48) can be shown to be χ^2_M distributed, when no model selection is performed. Whereas, corrections such as those discussed in Section 4.1, can be implemented as post-selection adjustments. Unfortunately, however, the asymptotic approximations are known to be rather slow in the parametric case. Therefore, in practical applications, when $G_{\mathbf{X}}$ depends on unknown parameters β , it is recommended to perform inference by means of the parametric bootstrap and which has been shown by Babu and Rao (2004) to be consistent also in the multivariate setting.

8 A diagnosis of background mismodelling

When conducting searches for new phenomena, mismodelling of the background distribution can dramatically compromise the sensitivity of the experiment. Specifically, overestimating the background can increase the chances of false negatives. Whereas, underestimating the background may lead to claiming false discoveries. To illustrate how iGOF can be used to understand if and how the postulated background model have been

misspecified, we consider a simulated observation by the Fermi Large Area Telescope (LAT) [Atwood et al. \(2009\)](#) obtained with the *gtobssim* package². The simulation includes a realistic representations of the instrumental noise of the detector and present backgrounds.

The region of interest corresponds to a disc in the sky of 30° radius and centered at (195 RA, 28 DEC), where RA and DEC are the coordinates in the sky. Here we assume that, despite the cosmic background is known to follow a uniform distribution over the search area, it is unclear if the instrumental error is effectively negligible, or if it has a prominent effect on the underlying distribution. Therefore, we set $G_{X_1 X_2}$ to be the cdf of a uniform distribution with support $\mathcal{X}_1 \times \mathcal{X}_2 = [165, 195] \times [28 - \sqrt{30^2 - (x - 195)^2}, 28 + \sqrt{30^2 - (x - 195)^2}]$ and we proceed by estimating the joint comparison density over a sample of $n = 68658$ observations. Specifically, we set $m_1 = m_2 = 4$ and we select the components of $\hat{\theta}$ via the BIC criterion in (30). The resulting estimate is

$$\hat{d}(G_1(x_1), G_2(x_2|x_1); G_{X_1 X_2}, F_{X_1 X_2}) = 1 + 0.0222T_1(G_1(x_1)) - 0.0427T_1(G_2(x_2|x_1)) + 0.0412T_2(G_2(x_2|x_1)). \quad (49)$$

In order to assess the significance of the deviations captured by (49), we compute both the confidence regions and deviance p-values via (34) and (32). The results are reported in the right panel of Figure 5, whereas the left panel shows the confidence regions and deviance p-value obtained via simulation. Similarly to what we have observed for Example I (see Figure 2), despite the approximate confidence bands are more conservative, they still allow to capture the main departures from uniformity. Indeed, in both cases, we can see that the prominent deviations of the true underlying model from the postulated uniform distribution occur in proximity of low values of X_2 . Whereas, at the center-left of the search area, the uniform model significantly underestimates the model inclusive of the instrumental error. Finally, it follows from (20) that an updated model background distribution which accounts for these deviations can be constructed by simply multiplying the uniform pdf by the estimated comparison density in (49).

9 Discussion

This work proposes an informative approach to goodness-of-fit which bridges exploratory and confirmatory data analysis to study multivariate distributions. The use of the joint comparison density allows practitioners to identify the sources of mismodelling, hence the informative character of the procedure. Specifically, confidence regions can be constructed as in Corollary 4.5 to identify regions of the parameter space where significant deviations occurs. While this approach is practical only for problems in at most three dimensions, in more dimensions a detailed diagnosis of mismodelling can be achieved by means of the iGOF-diagnostic analysis proposed in Section 6. It follows that confidence region plots and iGOF-diagnostic tables can be used to directly address Q1 in Section 1.

²<http://fermi.gsfc.nasa.gov/ssc/data/analysis/software>

An important step of the procedure proposed is the LP representation of the joint comparison density in (13). Specifically, the use of LP score functions allow us to generalize our methods to both discrete and continuous data. Furthermore, as highlighted in Section 5, iGOF reduces to an analysis of independence when replacing the Rosenblatt transform in Definition 2.1 with the empirical marginal distribution functions. This allow us to learn the underlying dependence structure of the data and visualize it through the dependence learning graph (see Section 5.2). Consequently, the latter can be used to directly address Q2 in Section 1.

As we aimed for when formulating Q3 in Section 1, the true probability function of the data can be estimated nonparametrically, when investigating the dependence structure, and semi-parametrically via (20), when assessing the validity of the model postulated by the scientists. Interestingly, in the latter case the resulting estimate incorporates the knowledge carried by the hypothesized knowledge and thus, it provides a data-driven update for it in the direction of the true distribution of the data.

Despite the usefulness of the methods presented here in applied settings, and in the physical sciences in particular (e.g., Section 8), they are not exempt from limitations. For instance, several problems in physics and astronomy, often involve no more than 8 or 10 dimensions and/or can be reduced to 2D planes (e.g., Aprile et al., 2017). In this context, choosing m_d equal to 3 or 4 for all $d = 1, \dots, p$, is often sufficient to avoid overfitting and, eventually, lack of power by implementing adequate model selection strategies and for sufficiently large samples (see Sections 4 and 6). In more dimensions, however, the method suffers from the curse of dimensionality (e.g. Friedman et al., 2001), as the size of the LP tensor basis increases exponentially fast with p . In this context, a regularized solution could be particularly valuable (see for instance Signoretto et al., 2014, in the context of tensor data analysis) when analyzing, for instance, data coming from large astronomical surveys such as the Large Synoptic Survey Telescope (LSST) survey (e.g., Tyson, 2002).

Finally, the post-selection inference approach presented in Section 4.1 enjoys wide generalizability and simple implementation. However, the adjustments proposed are, by construction, conservative. Despite this issue can, in principle, be overcome by simulation studies, in the most crucial (astro)physics discoveries the claim for a discover can only be made at a significance level of $3 \cdot 10^{-7}$ or lower (e.g., Lyons, 2013). Therefore, a numerical solution may be computationally prohibitive and an (asymptotically) exact post-selection inferential solution (see for instance Tibshirani et al., 2016, in the context of regression), could reduces drastically the computational complexity when dealing with stringent significant requirements.

Acknowledgments

The author thanks sincerely Estate V. Khmaladze and G. Jogesh Babu for the enlightening discussions and comments. Their valuable feedback has led to a substantial improvement of the quality and clarity of the manuscript.

References

- Adler, R. J. (2000). On excursion sets, tube formulas and maxima of random fields. *Annals of Applied Probability*, pages 1–74.
- Algeri, S. (2019). *TOHM: Testing One Hypothesis Multiple Times*. R package version 1.3.
- Algeri, S. (2020). Detecting new signals under background mismodeling. *Phys. Rev. D*, 101:015003.
- Algeri, S. et al. (2018). Statistical challenges in the search for dark matter. *arXiv:1807.09273*.
- Algeri, S. and van Dyk, D. A. (2020). Testing one hypothesis multiple times: the multidimensional case. *Journal of Computational and Graphical Statistics*, 29(2):358–371.
- Algeri, S. and Zhang, X. (2020). Smoothed inference and graphics via lp modeling. *arXiv preprint arXiv:2005.13011*.
- Aprile, E., Aalbers, J., Agostini, F., Alfonsi, M., Amaro, F., Anthony, M., Arneodo, F., Barrow, P., Baudis, L., Bauermeister, B., et al. (2017). First dark matter search results from the xenon1t experiment. *Physical review letters*, 119(18):181301.
- Atwood et al., W. B. (2009). The large area telescope on the fermi gamma-ray space telescope mission. *The Astrophysical Journal*, 697(2):1071.
- Babu, G. J. and Rao, C. R. (2004). Goodness-of-fit tests when parameters are estimated. *Sankhya*, 66(1):63–74.
- Balázs, C. et al. (2017). Colliderbit: a gambit module for the calculation of high-energy collider observables and likelihoods. *The European Physical Journal C*, 77(11):795.
- Barton, D. E. (1956). Neyman’s test of goodness of fit when the null hypothesis is composite. *Scandinavian Actuarial Journal*, 1956(2):216–245.
- Berk, R., Brown, L., Buja, A., Zhang, K., Zhao, L., et al. (2013). Valid post-selection inference. *The Annals of Statistics*, 41(2):802–837.
- Claeskens, G. and Hjort, N. L. (2004). Goodness of fit via non-parametric likelihood ratios. *Scandinavian Journal of Statistics*, 31(4):487–513.
- Cramér, H. (1999). *Mathematical methods of statistics*, volume 43. Princeton university press.
- Dauncey, P., Kenzie, M., Wardle, N., and Davies, G. (2015). Handling uncertainties in background shapes: the discrete profiling method. *Journal of Instrumentation*, 10(04):P04015.
- Friedman, J., Hastie, T., and Tibshirani, R. (2001). *The elements of statistical learning*, volume 1. Springer series in statistics New York.
- Kallenberg, W. C. M. and Ledwina, T. (1997). Data-driven smooth tests when the hypothesis is composite. *Journal of the American Statistical Association*, 92(439):1094–1104.
- Khmaladze, E. (2016). Unitary transformations, empirical processes and distribution free testing. *Bernoulli*, 22(1):563–588.
- Kolmogorov, A. (1933). Sulla determinazione empirica di una legge di distribuzione. *Inst. Ital. Attuari, Giorn.*, 4:83–91.
- Ledwina, T. (1994). Data-driven version of neyman’s smooth test of fit. *Journal of the American Statistical Association*, 89(427):1000–1005.
- Lyons, L. (2013). Discovering the Significance of 5 sigma. *arXiv:1310.1284*.
- Mardia, K. V. (1975). Assessment of multinormality and the robustness of hotelling’s t^2 test. *Journal of the Royal Statistical Society: Series C (Applied Statistics)*, 24(2):163–171.
- Mukhopadhyay, S. (2017). Large-scale mode identification and data-driven sciences. *Electronic Journal of Statistics*, 11(1):215–240.
- Mukhopadhyay, S. and Parzen, E. (2014). Lp approach to statistical modeling. *arXiv:1405.2601*.
- Mukhopadhyay, S. and Parzen, E. (2020). Nonparametric universal copula modeling. *Applied Stochastic Models in Business and Industry*, 36(1):77–94.
- Mukhopadhyay, S. and Wang, K. (2020). Nonparametric high-dimensional k-sample comparison. *Biometrika (to appear)*.
- Nelder, J. (1977). A reformulation of linear models. *Journal of the Royal Statistical Society: Series A (General)*, 140(1):48–63.
- Nelsen, R. B. (2007). *An introduction to copulas*. Springer Science & Business Media.
- Parzen, E. (1979). Nonparametric statistical data modeling. *Journal of the American statistical association*, 74(365):105–121.
- Parzen, E. (1983). Fun. stat quantile approach to two sample statistical data analysis. Technical report, Texas A&M University, College Station, Institute of Statistics.
- Parzen, E. (2004). Quantile probability and statistical data modeling. *Statistical Science*, 19(4):652–662.
- Priel, N., Rauch, L., Landsman, H., Manfredini, A., and Budnik, R. (2017). A model independent safeguard against background mismodeling for statistical inference. *Journal of Cosmology and Astroparticle Physics*, 2017(05):013.

- Rayner, J. C. W. and Best, D. J. (1990). Smooth tests of goodness of fit: an overview. *International Statistical Review/Revue Internationale de Statistique*, pages 9–17.
- Rayner, J. C. W., Thas, O., and Best, D. J. (2009). *Smooth tests of goodness of fit: using R*. John Wiley & Sons.
- Rosenblatt, M. (1952). Remarks on a multivariate transformation. *The annals of mathematical statistics*, 23(3):470–472.
- Signoretto, M., Dinh, Q. T., De Lathauwer, L., and Suykens, J. A. (2014). Learning with tensors: a framework based on convex optimization and spectral regularization. *Machine Learning*, 94(3):303–351.
- Smirnov, N. V. (1939). On the estimation of the discrepancy between empirical curves of distribution for two independent samples. *Bull. Math. Univ. Moscou*, 2(2):3–14.
- Taskinen, S., Oja, H., and Randles, R. H. (2005). Multivariate nonparametric tests of independence. *Journal of the American Statistical Association*, 100(471):916–925.
- Taylor, J., Takemura, A., Adler, R. J., et al. (2005). Validity of the expected euler characteristic heuristic. *The Annals of Probability*, 33(4):1362–1396.
- Taylor, J. E. and Worsley, K. J. (2008). Random fields of multivariate test statistics, with applications to shape analysis. *Ann. Statist.*, 36(1):1–27.
- Thas, O. (2010). *Comparing distributions*. Springer.
- Tibshirani, R. J., Taylor, J., Lockhart, R., and Tibshirani, R. (2016). Exact post-selection inference for sequential regression procedures. *Journal of the American Statistical Association*, 111(514):600–620.
- Tyson, J. A. (2002). Large synoptic survey telescope: overview. In *Survey and Other Telescope Technologies and Discoveries*, volume 4836, pages 10–20. International Society for Optics and Photonics.
- Vitells, O. and Gross, E. (2011). Estimating the significance of a signal in a multi-dimensional search. *Astroparticle Physics*, 35(5):230 – 234.
- Yellin, S. (2002). Finding an upper limit in the presence of an unknown background. *Physical Review D*, 66(3):032005.